COMPOSITE EXPANSION OF ACTIVE AND INACTIVE MOTIONS OF THE STREAMWISE REYNOLDS STRESS

Ronald L. Panton
Mechanical Engineering Department
University of Texas
1 University Station, C 2200
Austin, Texas 78712
rpanton@mail.utexas.edu

ABSTRACT

Fluctuations of the streamwise velocity are considered as a sum of active and inactive parts. The active and inactive components of the streamwise Reynolds stress are assumed to scale differently. Because the active motions produce Reynolds shear stress, the active component is further assumed to be proportional to the Reynolds shear stress. This allows DNS data can be used to compute the inactive component. A model of the inactive motion in the inner and outer layers is proposed and a composite expansion formulated. The composite expansion of the inactive component, together with a previous composite expansion of the Reynolds shear stress, allows the streamwise Reynolds stress to be predicted as a function of wall distance and Reynolds number. According to the model the streamwise Reynolds stress is dominated by the inactive component. This domination increases as the Reynolds number increases.

INTRODUCTION

Consider the fully developed turbulent flow in a pipe or channel where the wall to centerline distance is h and the fluid viscosity is ν. The mean velocity is $U(y)$ where y is the distance from the wall. The streamwise direction is x, the spanwise direction z, and u, v, w are the fluctuation velocity components. Velocity scales are U_0 , the centerline velocity, and u_* , the friction velocity. The Reynolds shear stress $-<u\mathrm{v}>$ correlates (is independent of Re_*) when scaled with u_* ;

$$< u\mathrm{v} >^+ \equiv < u\mathrm{v} > /u_*^2 \tag{1}$$

However, in the last few years data has shown that the streamwise Reynolds stress $<uu>$ does not scale with u_*.

$$< uu >^+ \equiv < uu > /u_*^2 \tag{2}$$

This lack of scaling is illustrated in Fig.1 which displays DNS data (Del Almo anf Jinenez (2003), Del Almo et al(2004), Moser et al.(1999)) at several Reynolds numbers.

Townsend (1976) proposed that the streamwise fluctuations consisted of two categories of motion; active and inactive. That concept is employed herein with the additional assumption that these motions scale differently. Since wall turbulence has a two layer structure, a correlating function is proposed for each motion in each region. Reynolds number effects are predicted by a composite expansion for each category of motion. The initial discussion of these ideas are found in Panton (2007). After a review of the formulation of the composite expansions, this paper will investigate the effect of varying several arbitrary parameters. One parameter, α, controls scaling the inactive component. The other,P, is a measure of the strength of the active component.

Proper correlation of $< uu >$ is important because the streamwise fluctuations have a close association with the fluctuating wall shear stress, the fluctuating wall pressure, and the turbulent kinetic energy.

ACTIVE AND INACTIVE MOTIONS

Townsend's concept of inactive motion has been interpreted, extended, and modelled by several researchers in the past. Noteworthy papers are: Perry and Abell (1977), Perry and Chong (1982), Perry et al. (1986), and Maursic et al. (1997). Marusic and Kunkel (2003), produced equations representing inactive effects in boundary layers for all distances. In these papers the $< uu >$correlation is completely inactive motions that are attributed to attached wall eddies. Townsend (1976) himself envisioned that the inactive motion was a stramwise-spanwise motion contributing to u and w fluctuations. He chose the term "inactive" motion envisioning that it makes no essential contribution to the Reynolds shear stress.

All Reynolds stresses are time-averaged quantities. As such, certain instantaneous fluctuation motions average out and make no essential contribution to the final values.

There are two distinct velocities that one can use for scaling wall turbulence quantities; U_0 and u_*. As the Reynolds number increases $u_* / U_0 \to 0$ and these quantities separate. There are other choices, however, they are asymptotically equivalent. For example U_{ave} is equivalent to U_0 or $U_0 - U_{ave} \sim u_*$ (the Zagarola-Smits scale) is equivalent to u_*. Use of these alternate scales may extend a correlation to lower Reynolds numbers, and in this sense are better, but they are not fundamentally different.

The Reynolds shear stress correlates with u_* as a scale. A composite expansion for $< u\mathrm{v} >^+ \equiv < u\mathrm{v} > /u_*^2$ represents the data for all wall distances to remarkible low values of the Reynolds numbers. Thus, active motions will scale with u_*. Inactive motions, by difinition do not make an esssential contribution to the Reynolds shear stress. Physically they are associated with eddies of the outer region. The mean velocity in this region is, to zeroth order, U_0, while vertical velocity fluctuations are of order u_*. Eddies are restrained in the normal direction by the wall; however, they are not restrained in the streamwise direction. It is not unreasonable to imagine that the scaling of the inactive motions is some combination of u_* and U_0. In fact, Degraaff and Eaton (2000) propose that the so-called mixed scaling $\sqrt{U_0\, u_*}$, introduced by Alfredsson and Johnsson (1984), is the proper scale for $< uu >$.

The peak values on Fig. 1 always occur at about y+ = 15, and are plotted along with some experimental measurements as a function of U_0 / u_* in Fig. 2 . The points on Fig. 2 at very high values of U_0 / u_* are atmospheric boundary layer measurements of Metzger and Klewicki (2001). A dashed line on this figure has a slope of one and corresponds to the Degraaff and Eaton(2000) scaling. The peak values are in the inner layer. Data from the outer layer at *Y = 0.4* are plotted in Fig. 3. An upward trend is again observed, however, because of the scatter in experimental data, the trend conuld be interpreted differently. It should be noted that hot wire resolution issues are not completely resolved. Figures 1, 2, and 3 offer strong evidence that $< uu >^+$ is not scaled properly to be independent of Reynolds number.

Properties of Active and Inactive Motions

To motivate a scaling law, let the streamwise velocity be an active motion u_A plus an inactive motion u_I.

$$u = u_I + u_A \qquad (3)$$

It is not necessary to make a unique instataneous definition. As discussed above, active motions make an essential contribution to the Reynolds shear stress <*u*v>, while inactive motions do not. Another viewpoint would be that u_I and v are statistically independent. The correlation of two statistically independent quantities is the product of their mean values. Because the mean $< \mathrm{v} >$ is zero,

$$< u_I \mathrm{v} > = < u_I >< \mathrm{v} > = 0 \qquad (4)$$

Thus, the Reynolds stress in entirely active *u* motions in agreement with the Towsend concept.

$$< u\mathrm{v} > = <(u_A + u_I)\,\mathrm{v} > = < u_A \mathrm{v} > \qquad (5)$$

Note that the mean of $< u >$ is zero, but it is possible that the component motions have nonzero means.

$$< u_I > = - < u_A > \qquad (6)$$

One would be negative and the other positive.

SCALING THE <uu> REYNOLDS STRESS

The streamwise Reynolds stress correlation consists of an active part, inactive part, and a cross correlation of active and inactive parts.

$$< uu > = < u_I u_I > + 2 < u_I u_A > + < u_A u_A > \qquad (7)$$

Assuming that u_I and u_A are statistically independent, the cross-correlation is equal to the product of the individual means, thus inserting Eq. 6 gives

$$< uu > = < u_I u_I > - 2 < u_A >^2 + < u_A u_A > \qquad (8)$$

Let us consider the proper scaling for each term in Eq. 8

Active motions are associated with the Reynolds shear stress and therefore one would anticipate that $< u_A u_A >$ would have the same scaling as $- < u\mathrm{v} >$. Define

$$< u_A u_A >^+ \equiv < u_A u_A > / u_*^2 \qquad (9)$$

Scaling with u_* will produce an order one quantity for limit $\mathrm{Re}_* \to \infty$.

Similarly the mean of the active motion is scaled with u_*.

$$< u_A >^{+2} \equiv < u_A >^2 / u_*^2 \qquad (10)$$

If this scaling is incorrect then a factor $\left(u_* / U_0\right)^\beta$ needs to be inserted on the right side of Eq. 10.

It has been established experimentally, DeGraff and Eaton (2000) and Metzger and Klewicki (2001) and by DNS, Del Álamo and Jimenez (2003) that $< uu >$ does not scale simply with u_*. Figure 2 illustrates this as $< uu >^+ \equiv < uu > / u_*^2$ is plotted vs U_0 / u_*. Maximum values (in the inner region at about y$^+$ = 15) and values at $Y = y / h = 0.4$ (in the outer region) continue to increase with increasing U_0 / u_* (increasing Re$_*$). Let α be an exponent that gives an order one quantity in the limit $\mathrm{Re}_* \to \infty$.

$$< uu >^\# \equiv \frac{< uu >}{u_*^2}\left(\frac{u_*}{U_0}\right)^\alpha = < uu >^+ \left(\frac{u_*}{U_0}\right)^\alpha \qquad (11)$$

The scaling of Degraaff and Eaton (2000) is $\alpha = 1$.

In the limit $\mathrm{Re}_* \to \infty$ the nondimensional form of Eq. 8 must have one term on the right side to balance the left side. This can only be the inactive motion. Therefore $< u_I u_I >$ has the same scaling as Eq. 11.

$$< u_I u_I >^\# \equiv < u_I u_I >^+ \left(\frac{u_*}{U_0}\right)^\alpha \qquad (12)$$

To be of order one for limit $\mathrm{Re}_* \to \infty$, the terms in Eq. 59 need different scalings.

With the definitions, Eqs. 9-12, the nondimensional form of Eq.9 is

$$\langle uu\rangle^{\#} = \langle u_I u_I\rangle^{\#} - \left(2\langle u_A\rangle^{+2} - \langle u_A u_A\rangle^{+}\right)\left(\frac{u_*}{U_0}\right)^{\alpha} \quad (13)$$

At high Reynolds numbers the inactive motions dominate $\langle uu\rangle$.

DATA ANALYSIS PROCEDURE

Regardless of the physical interpretation of Eq. 13, one can, in complete generality, propose an asymptotic expansion of the form,

$$\langle uu\rangle^{\#} = f_O(y) + f_1(y)\left(\frac{u_*}{U_0}(\mathrm{Re}_*)\right)^{\alpha} \quad (14)$$

The power α is chosen to make the definition in Eq. 11 of order one. The form of Eq 14 is proposed for both the inner and outer regions. If the same power α occurs for both regions, that is, if there is no change in scaling of $\langle uu\rangle^{\#}$, then the common part of the inner and outer functions is a constant.

In order to evaluate the usefulness of Eq. 13, we will insert data for $\langle uu\rangle^{\#}$, model the terms $\left(2\langle u_A\rangle^{+2} - \langle u_A u_A\rangle^{+}\right)$, and solve for the inactive correlation $\langle u_I u_I\rangle^{\#}$. Success is achieved if $\langle u_I u_I\rangle^{\#}$ is independent of Reynolds number as $\mathrm{Re}_* \to \infty$.

By definition the active motions are essential to the Reynolds shear stress. Assume that the correlation is some constant M times the Reynolds shear stress.

$$\langle u_A u_A\rangle^{+} = -M\langle uv\rangle^{+} \quad (15)$$

Since $\langle uv\rangle^{+}$ is negative, M is positive. Also assume that the active mean is some number N times the Reynolds shear stress.

$$-2\langle u_A\rangle^{+2} = -2N\langle uv\rangle^{+} \quad (16)$$

The constant N is negative. The combination $2N + M = P$ is negative (-1) for $M=1$, $N=-1$.

With these assumptions Eq. 13 becomes

$$\langle u_I u_I\rangle^{\#} = \langle uu\rangle^{\#} - P\left(-\langle uv\rangle^{+}\right)\left(\frac{u_*}{U_0}\right)^{\alpha} \quad (17)$$

For pipes and channels a composite expansion model predictes the Reynolds shear stress and its dependency on y and Re_* (Panton 2005). The relation is

$$-\langle uv\rangle^{+} = \frac{2}{\pi}\tan^{-1}\left(\frac{2\kappa y^{+}}{\pi}\right)\left[1-\exp\left(-\frac{y^{+}}{C^{+}}\right)\right] - \frac{y^{+}}{\mathrm{Re}_*} \quad (18)$$

For calculations herein the constants were taken as $\kappa = 0.37$, $C^{+} = 6.78$.

A major effort of this paper will be to investigate the trends for various choices of the parameters P and α. in Eq.17. The DNS data will be processed because it has much more internal consistency than experimental data. A disadvantage of the DNS data is that the Reynolds numbers are low . At only the highest Reynolds number, $\mathrm{Re}_* = 2003$, or perhaps the highest two values, 2003 and 935, is there minimal interaction between inner and outer layers.

Equation 17 is used to calculate the inactive component $\langle u_I u_I\rangle^{\#}$ by inserting DNS data for $\langle uu\rangle^{\#}$, choosing $\alpha = 1$, $P = -1$, and employing Eq. 13 to compute the Reynolds shear stress. Both the total and inactive components are shown in Fig. 4 as a function of the outer variable Y. A slightly better collapse on the inactive component is observed, especially at the higher Reynolds numbers. The inactive stress will be represented by a composite expansion.

$$\langle u_I u_I\rangle^{\#}_{Comp}(y^{+}, \mathrm{Re}_*) = \langle u_I u_I\rangle^{\#}_{In}(y^{+}) + \langle u_I u_I\rangle^{\#}_{Out}(Y \quad y^{+}/\mathrm{Re}_*) - \langle u_I u_I\rangle^{\#}_{cp} \quad (19)$$

The sum of an inner law, an outer law, minus the common part gives a representation that shows Reynolds number dependence and is uniformly valid.

An equation was chosen to represent the outer data. That is, the trends of Fig. 4 excluding the behavior near $Y=0$.

$$\langle u_I u_I\rangle^{\#}_{Out} = (C_{cp} - C_{cl})\left[1-Y\right]^{3/2} + C_{cl} \quad (20)$$

The centerline value is C_{cl}, and the common part at $Y = 0$ is $\langle u_I u_I\rangle^{\#}_{cp} = C_{cp}$. Values from Fig. 4 are $C_{cp} = 0.245$ and $C_{cl} = 0.033$.

The same equation might not apply to pipe or boundary layers flows because those flows have different velocity wake components and, in the case of a boundary layer, a different $-\langle uv\rangle$ correlation.

The inner region is correlated by solving Eq. 19 for the inner function.

$$\langle u_I u_I\rangle^{\#}_{In} = \langle u_I u_I\rangle^{\#} - \left(\langle u_I u_I\rangle^{\#}_{Out} - \langle u_I u_I\rangle^{\#}_{cp}\right) \quad (21)$$

Equation 20 gives the term in brackets, and DNS data is used for the $\langle u_I u_I\rangle^{\#}$. Figure 5 displays the results. There is a slight shift in the peak with Re_* that is not represented by this level of approximation. The data at $\mathrm{Re}_* = 2000$ was approximated by the equation.

$$\langle u_I u_I\rangle^{\#}_{In} = C_0\left[1-\exp\left(-\frac{y^{+}}{C_1}\right)\right]^2 - \left(C_0 - C_{cp}\right)\left[1-\exp\left(-\frac{y^{+}}{C_2}\right)\right] \quad (22)$$

$C_0 = 0.724$; $C_1 = 5.41$; $C_2 = 18.3$

RESULTS

The inactive streamwise stress computed as described above with values of α = 7/8, 1, and 9/8 and values of *P*= -0.5, -1, and -1.5 are given in Figs. 6 and 7. A good result is indicated if the curves become flat as U_0 / u_* increases. Figure 6 gives the peak values in the inner region, and Fig. 7 displays values in the outer region at *Y = 0.4*. The value of *P* indicates the amount of active motion that is subtracted fron the total streamwise stress in order to produce the inactive portion. Different *P* values shift the curves, but do little to change the shape or improve the correlations.

On the other hand, the values of α, the scaling coonstant, Eq. 11, show a stronger effect on the shape of the curves. On Fig. 7 α= 9/8 produces the flattest curves at high Reynolds numbers (high U_0 / u_*), although α= 1 is relatively satisfactory.

Fitting the DNS <uu> data at Re_* = 2003, to yield constants for Eqs. 20 and 22 yields a model with which one can predict the the curvse for any Reynolds number. Figure 8 shows the trend of the peak values and the values at *Y = 0.4*. as functions of U_0 / u_*. For this figure the value *P = -1* was assumed and various values of alpha investigated. All curves crossa together at $U_0 / u_* = 24.3$ because this is the fitting point at Re_* = 2003. For purposes of comparison the alpha = 1 curves from this figure are also plotted on Figs. 2 and 3. The scatter displayed in the data of Figs. 1 and 2 does not reveal a preferred value for alpha.

The last figure, Fig.9 displays the model predictions of a composite expansion, (α = 1, *P = – 1*) for <uu> , scaled in the traditional way with u_*, for various Reynolds numbers. The trends mimic the trends in DNS and experimental data. The curves for the highest an lowest Reynolds numbers, $Re_* = 186 \text{ and } 10^5$, also have the inactive component plotted. From the inactive component the active part is subtracted, it is negative, to yield the total stress. The active component is always a small part of the total. At the peak it subtracts about 0.5 from values from 6.5 to 13. In the middle of the outer layer the active part takes on ist largest value about one.

SUMMARY

Townsend's idea of active and inactive turbulent fluctuations was applied to the streamwise Reynolds stress <uu> with the assumption that the components scale differently. Active motions scale as $< u_A u_A > / u_*^2$ while inactive motions scale as $< u_I u_I > / (u_*^{2-\alpha} U_0^{\alpha})$. Mixed scaling is $\alpha = 1$. Using DNS data and assuming that the active motions are proportional, with constant *P*, to the Reynolds shear stress, a composite expansion is constructed for the inactive stress. Without further refinement of the experimental data or extension of DNS to higher Reynolds numbers, the choices $\alpha = 1$ and *P= -1* appear satisfactory. A composite model of the total stress <uu> illustrates the proper trends. It also shows that inactive motions dominate the streamwise stress, and that they become more prominent as the Reynolds number increases.

REFERENCES

Christensen, K. T. & Adrian, R. J. 2001 Statistical evidence of hairpin vortices in wall turbulence, *J. Fluid Mech*. **431** pp 433-443.

Carlier, J. & Stanislas, M. 2005 "Experimental study of eddy structures in a turbulent boundary layer using PIV," *J. Fluid Mech.* **535**, pp143-188.

Del Álamo, J. C. & Jimenez, J. 2003 Spectra of very large anisotropic scales in turbulent channels. *Phy. Fluids* **15** pp L41-L44.

Del Álamo, J. C. Jimenez, J. Zandonade, P. & Moser, R. D. 2004 Scaling the energy spectra in turbulent channels. *J. Fluid Mech.* **500**, pp135-144.

DeGraff , D. B. & J. K. Eaton 2000 "Reynolds number scaling of the flat plate turbulent boundary layer," *J. Fluid Mech.* **422**, pp319-346.

Harder, K. J. & Tiederman, W. G. 1991, "Drag reduction and turbulent structure in two-dimensional channel flow," *Phil.Trans. Roal. Soc*. Series A, Vol. **336**, pp19-28.

Hoyas,S. & Jimenez, J. 2005, "Scaling the velocity fluctuations in turbulent Channels up to Re_Q= 2003," Annual Research Briefs-2005, Center for Turbulence Research, pp 351-356.

Johansson, A. V. & Alfredsson, P. H. 1983 "Effects of imperfect spatial resolution on measurements of wall-bounded turbulent shear flows," *J. Fluid Mech.* **137**, pp409.

Maursic , I. Uddin, A. & Perry, A. 1997 "Similarity law for the streamwise turbulence intensity in zero-pressure-gradient turbulent boundary layers," *Phys. Fluids* **9** p3718.

Marusic , I. & Kunkel, G. J. 2003 "Streamwise turbulent intensity formulation for flat-plate boundary layers," *Phys. Fluids* **15**, pp2461-2464.

McKeon, B. J. Li, J. Jiang, W. .Morrison, J. F. & Smits, A. J. 2004 Further observations on the mean velocity distribution in fully developed pipe flow," *J. Fluid Mech.* **501**, pp135-147.

Metzger. M. M. Klewicki, J. C. Bradshaw , K. L. & Sadar, R. 2001 "Scaling the near-wall turbulent stress in the zero pressure gradient boundary layer," *Phys. Fluids*, **13**, pp1819-1821.

Metzger. M. M. & Klewicki 2001 "A comparative study on near-wall turbulence in high and low Reynolds number boundary layers ," *Phys. Fluids*, **13**, pp692-701.

Morrison, J. F. MeKeon, B. J. Jiang, W. & Smits, A. J. 2004 " Scaling the streamwise velocity component in turbulent pipe flow," *J. Fluid Mech.* **508**, pp 99-131.

Moser, R. D. Kim, J. Mansour, N. N. 1999 "Direct numerical simulation of turbulent channel flow up to Re_tau = 590," *Phys. Fluids*, **11**, p 943.

Nagib, H. M. & M. H. Hites 1995 AIAA paper 95-0786 .

Panton, R. L. 1997 "A Reynolds stress function for wall layers," Journal of Fluid Engineering, **119**, pp 325.

Panton, R. L. 2005 "Review of wall turbulence as described by composite expansions," *Applied Mechanics Reviews*, **58**, pp 1-36.

Perry, A. E. & Abell, C. J. 1977 "Asymptotic similarity of turbulence structures in smooth- and rough-walled pipes, *J. Fluid Mech.* **79**, pp 785-799.

Perry, A. E. Henbest, S. & Chong, M. S. 1986 "A theoretical and experimental study of wall turbulence, *J. Fluid Mech.* **165**, pp 163-199.

Townsend, A. A. 1976 *The Structure of Turbulent Shear Flow* Cambridge University Press. second edition

Wei, T. & Willmarth, W. W. 1989 *Reynolds Number Effects on the Structure of a Turbulent Channel Flow J. Fluid Mech.* **204**, pp 57-64.

Zagarola, M. V. & A. J. Smits 1998 "Mean flow scaling of turbulent pipe flow," *J. Fluid Mech.* 373, 33-79.

Zanoun, E. Nagib, H. Durst, F. & P. Monkewitz 2002 "Higher Reynolds number channel data and their comparison to recent asymptotic theory," AIAA 2002-1102.

Zanoun, E.-S. 2003 "Answers to some open questions in wall-bounded laminar and turbulent shear flows," PhD thesis, Inst. Fluid Mech. Friedrich-Alexander University of Erlangen-Nuremberg.

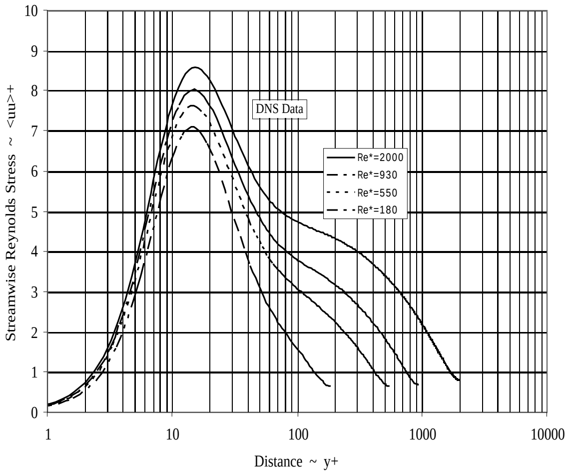

Figure 1. Streamwise Reynolds stress for several Reynolds numbers. DNS data

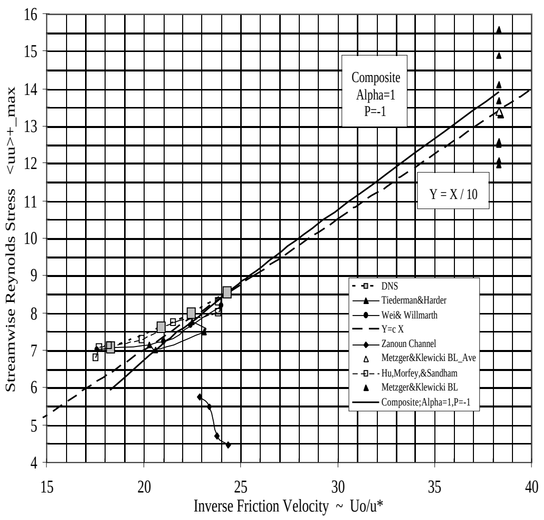

Figure 2. Maximum Streamwise Reynolds stress for experiments and DNS. See references for sources.

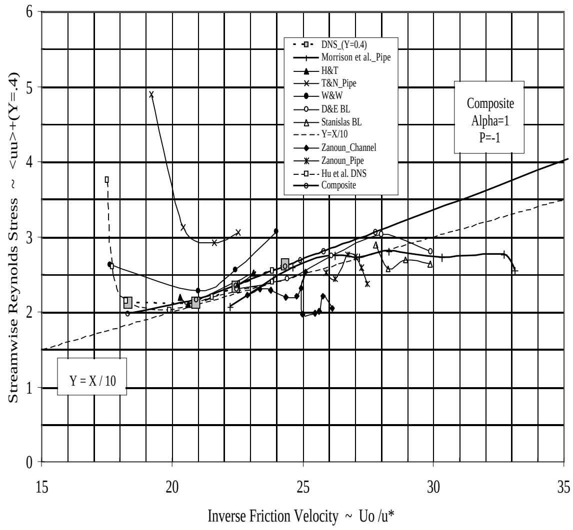

Figure 3. Streamwise Reynolds stress in the outer region, Y=0.4, for experiments and DNS.

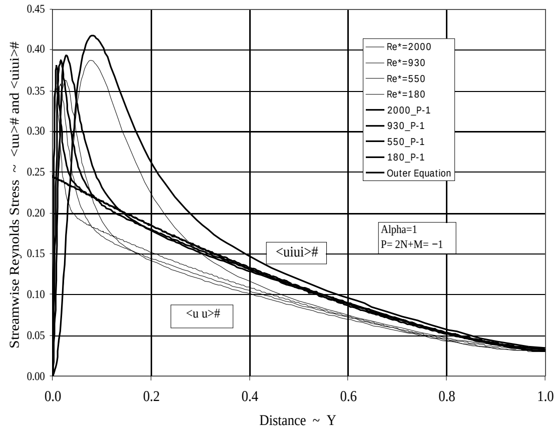

Figure 4.Total and inactive streamwise Reynolds stress for several Reynolds numbers. Based on DNS data.

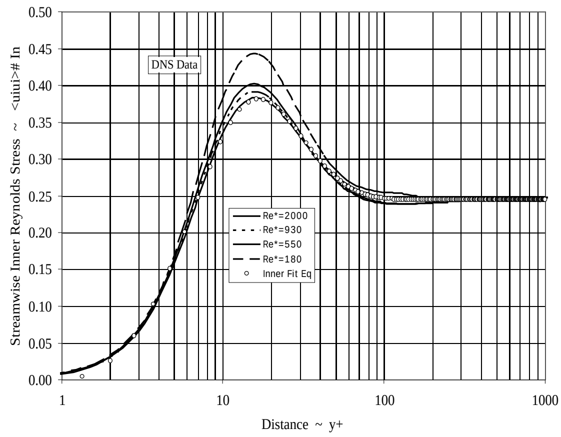

Figure 5 Inner inactive streamwise Reynolds stress for several Reynolds numbers. Based on DNS data.

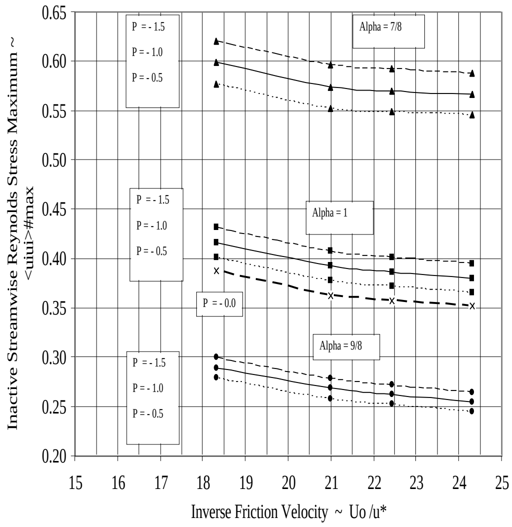

Figure 6. Maximum Inactive Reynolds stress for various P values (active parts). Based on DNS data.

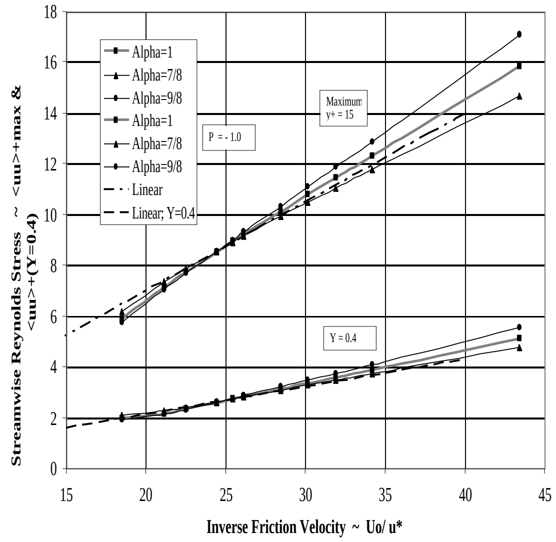

Figure 8. Composite streamwise Reynolds stress in traditional inner scaling for various alpha.

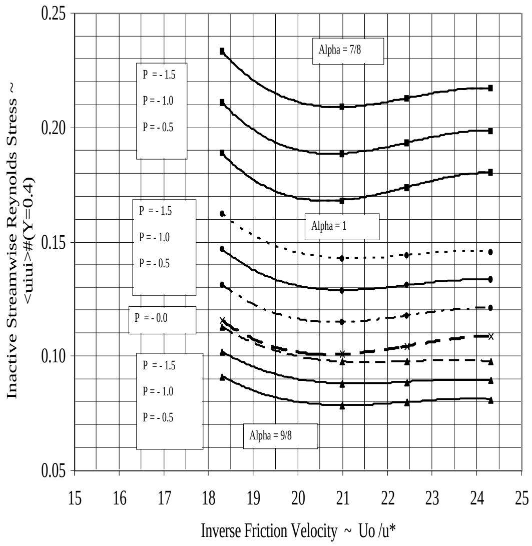

Figure 7. Inactive streamwise stress in outer region for various P values. Based on DNS data.

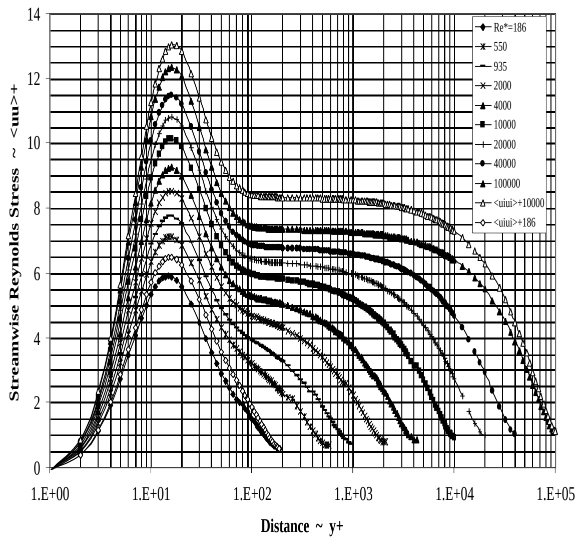

Figure 9 Composite of streamwise Reynolds stress. Open symbols at Re*=186 and 10^5 are inactive stresses.